








OPEN

Discovery of a colossal slickhead (Alepocephaliformes: Alepocephalidae): an active-swimming top predator in the deep waters of Suruga Bay, Japan

Yoshihiro Fujiwara^{1,11}[✉], Masaru Kawato^{1,11}, Jan Yde Poulsen², Hitoshi Ida³, Yoshito Chikaraishi^{4,5}, Naohiko Ohkouchi⁵, Kazumasa Oguri¹, Shinpei Gotoh⁶, Genki Ozawa^{1,7}, Sho Tanaka⁸, Masaki Miya⁹, Tetsuya Sado⁹, Katsunori Kimoto¹, Takashi Toyofuku¹⁰ & Shinji Tsuchida¹

A novel species of the family Alepocephalidae (slickheads), *Narcetes shonanmaruae*, is described based on four specimens collected at depths greater than 2171 m in Suruga Bay, Japan. Compared to other alepocephalids, this species is colossal (reaching ca. 140 cm in total length and 25 kg in body weight) and possesses a unique combination of morphological characters comprising anal fin entirely behind the dorsal fin, multiseriate teeth on jaws, more scale rows than congeners, precaudal vertebrae less than 30, seven branchiostegal rays, two epurals, and head smaller than those of relatives. Mitogenomic analyses also support the novelty of this large deep-sea slickhead. Although most slickheads are benthopelagic or mesopelagic feeders of gelatinous zooplankton, behavioural observations and dietary analyses indicate that the new species is piscivorous. In addition, a stable nitrogen isotope analysis of specific amino acids showed that *N. shonanmaruae* occupies one of the highest trophic positions reported from marine environments to date. Video footage recorded using a baited camera deployed at a depth of 2572 m in Suruga Bay revealed the active swimming behaviour of this slickhead. The scavenging ability and broad gape of *N. shonanmaruae* might be correlated with its colossal body size and relatively high trophic position.

Marine environments are increasingly being affected by global climate change and anthropogenic activities, leading to oceanic warming, acidification, and deoxygenation even in deep-sea regions¹. Such global changes are assumed to initially affect large, predatory consumers and subsequently have repercussions for organisms at lower trophic levels². There is thus an urgent need to elucidate the present biodiversity and abundance of predatory fishes inhabiting deep-sea sites³.

¹Research Institute for Global Change, Japan Agency for Marine-Earth Science and Technology (JAMSTEC), Yokosuka, Kanagawa, Japan. ²Fish Section, Australian Museum, Sydney, NSW, Australia. ³School of Marine BioSciences, Kitasato University, Sagami-hara, Kanagawa, Japan. ⁴Institute of Low Temperature Science, Hokkaido University, Sapporo, Hokkaido, Japan. ⁵Research Institute for Marine Resources Utilization, Japan Agency for Marine-Earth Science and Technology (JAMSTEC), Yokosuka, Kanagawa, Japan. ⁶Department of Marine Electronics and Mechanical Engineering, Tokyo University of Marine Science and Technology, Koto-ku, Tokyo, Japan. ⁷TechnoSuruga Laboratory Co., Ltd., Shizuoka, Shizuoka, Japan. ⁸Department of Marine Biology, Tokai University, Shizuoka, Shizuoka, Japan. ⁹Department of Ecology and Environmental Sciences, Natural History Museum and Institute, Chiba, Chuo-ku, Chiba, Japan. ¹⁰Institute for Extra-cutting-edge Science and Technology Avant-garde Research (X-star), Japan Agency for Marine-Earth Science and Technology (JAMSTEC), Yokosuka, Kanagawa, Japan. ¹¹These authors contributed equally: Yoshihiro Fujiwara and Masaru Kawato. ✉email: fujiwara@jamstec.go.jp

In 2016, we conducted bottom longline surveys and in situ camera observations in Suruga Bay, Japan, with the aim of obtaining information on the faunal diversity and trophic interactions of deep-sea predatory fishes. Suruga Bay, which is the deepest bay in Japan (maximum depth: ca. 2500 m), is located in the central region of the Pacific coastline of the Japanese Archipelago. Since the late 1800s, natural history studies have been conducted in this bay and the fauna inhabiting the bay have accordingly been well documented^{4–9}. Commercial deep-sea trawl, bottom longline, and baited pot fishing have been actively conducted in this bay and tons of predatory fish are caught annually. As such, in terms of gaining an understanding of the vulnerability of deep-sea ecosystems to anthropogenic impacts, Suruga Bay represents an ideal research location for constructing dynamic ecosystem models that incorporate large predators.

The genus *Narctes* Alcock, 1890, is a member of the family Alepocephalidae (slickheads), consisting of three named species, i.e., *N. erimelas*, *N. lloydi*, and *N. stomias*¹⁰. The members of this genus are bathypelagic, inhabiting depths between 700 and 2600 m, and are distributed globally. They reach approximately 75 cm in standard length. This genus is characterized by multiserial teeth on premaxillary and dentary, laterally expanded dentary with a toothless area at symphysis. The members have 26–33 precaudal vertebrae and 18–25 caudal vertebrae (48–56 in total), with 3–14 more precaudal than caudal vertebrae, relatively large centra spaces for the spinal cord, 8–14 long pyloric caeca, generally 8 branchiostegal rays, and 3–6 + 1 + 10–17 gill rakers on the first arch¹¹. Sazonov¹⁰ reviewed all species of the genus and synonymized *Bathytroctes alveatus* Garman, 1899 with *N. erimelas* Alcock, 1890 and *N. kamoharai* Okamura, 1984 and *N. wonderi* Herre, 1935 with *Narctes lloydi* Fowler, 1934.

Surprisingly, during our surveys, we captured four individuals belonging to an extraordinarily large, unidentified *Narctes* species from a region deeper than 2171 m at the opening of the bay. Although fishes in the order Alepocephaliformes are widely distributed in the world's oceans and comprise a diverse group of deep-sea fishes^{11–13}, their biology and systematics remain poorly understood, owing largely to the infrequent surveying of their deep habitats.

Here, we describe a novel slickhead species of the genus *Narctes* and present detailed morphological descriptions, along with the results of X-ray computed tomography (CT), molecular phylogeny, and stable isotope analyses. This species described here is the largest alepocephalid fish reported to date and is one of the largest bathyal species of bony fish ever described, reaching ca. 140 cm in total length and ca. 25 kg in weight. The noteworthy trophic position, diet, and swimming behaviour of the newly discovered species are also reported.

Results

Bottom longline sampling. Four individuals of an alepocephalid species were collected from Suruga Bay using a bottom longline installed on the training vessel *Shonan maru* (SH) belonging to the Kanagawa Prefectural Marine Science High School. The first two individuals were collected at depths of 2171 m and 2179 m on 4th February 2016 during the cruise SH16-01, and the other two specimens were captured at depths of 2572 m and 2551 m on 23rd November 2016 during the cruise SH16-02 (Fig. 1, Table 1). The total lengths of the fish ranged from 122 to 138 cm (Table 1). The two individuals collected during the SH16-01 cruise were fixed with formalin as the holotype (sample ID: SH8-69) and paratype 1 (sample ID: SH8-43). The remaining two individuals (sample IDs: SH12-1 and SH12-14) collected during the SH16-02 cruise were frozen and were also deposited as paratypes 2 and 3, respectively (Table 1).

Systematics. Family Alepocephalidae Bonaparte, 1846.

Genus *Narctes* Alcock, 1890.

Narctes shonanmaruae sp. nov. Poulsen, Ida, Kawato & Fujiwara (Figs. 2 and 3, Tables 1 and 2, Supplementary Figs. S1–S16) (proposed English name: Yokozuna Slickhead, proposed Japanese name: Yokozuna Iwashi).

Material. Holotype: JAMSTEC No. 1160053133 (Sample ID: SH8-69), 121.0 cm SL, female, Suruga Bay, 2171 m depth, 4th February 2016, collected by YF, GenBank No. AP018429.

Paratypes: (1) KPM-NI 43548 (Sample ID: SH8-43), 104.0 cm SL, female, Suruga Bay, 2179 m depth, 4th February 2016, collected by YF, GenBank No. AP018430; (2) NSMT-P 132616 (Sample ID: SH12-1), 111.5 cm SL, female, Suruga Bay, 2572 m depth, 23rd November 2016, collected by YF, DDBJ No. LC409533; (3) CBM-ZF-0019048 (Sample ID: SH12-14), 117.5 cm SL, female, Suruga Bay, 2551 m depth, 23rd November 2016, collected by YF, DDBJ No. LC409534. The holotype and three paratypes provided genotypes according to Chakrabarty et al.¹⁴. This published study and the nomenclatural acts it contains have been registered in ZooBank, the online registration system for the ICZN. The ZooBank LSIDs (Life Science Identifiers) can be resolved and the associated information viewed through any standard web browser by appending the LSID to the prefix "<http://zoobank.org/>". The LSID for this publication is: urn:lsid:zoobank.org:act:7C56487C-7E3F-4096-ACED-171DCD90C4D0.

Species diagnosis. Anal fin entirely behind the dorsal fin. Teeth on premaxillary, maxillary, and dentary multiserial. Predorsal scale rows greater than 70. Longitudinal scale rows greater than 110. Dorsal to lateral line scale row greater than 15. Anal to lateral line scale rows greater than 17. Branchiostegal rays 7. Dorsal-fin rays less than 15. Precaudal vertebrae less than 30. Epurals 2. Lengths of head, snout, upper and lower jaws, orbit diameter, dorsal and anal fin bases relatively short against standard length (SL).

Description (Figs. 2, 3, Tables 1, 2, Supplementary Figs. S1–S16). General appearance (Figs. 2a–c, Supplementary Figs. S1, S2, S16): Body relatively long, fusiform, more or less laterally compressed, head robust and broad, body colour purplish, black pores scattered on head; skull and head region without scales; dorsal-fin base anterior to origin of anal fin base non-overlapping in vertical direction; dorsal-fin base slightly posterior to pelvic

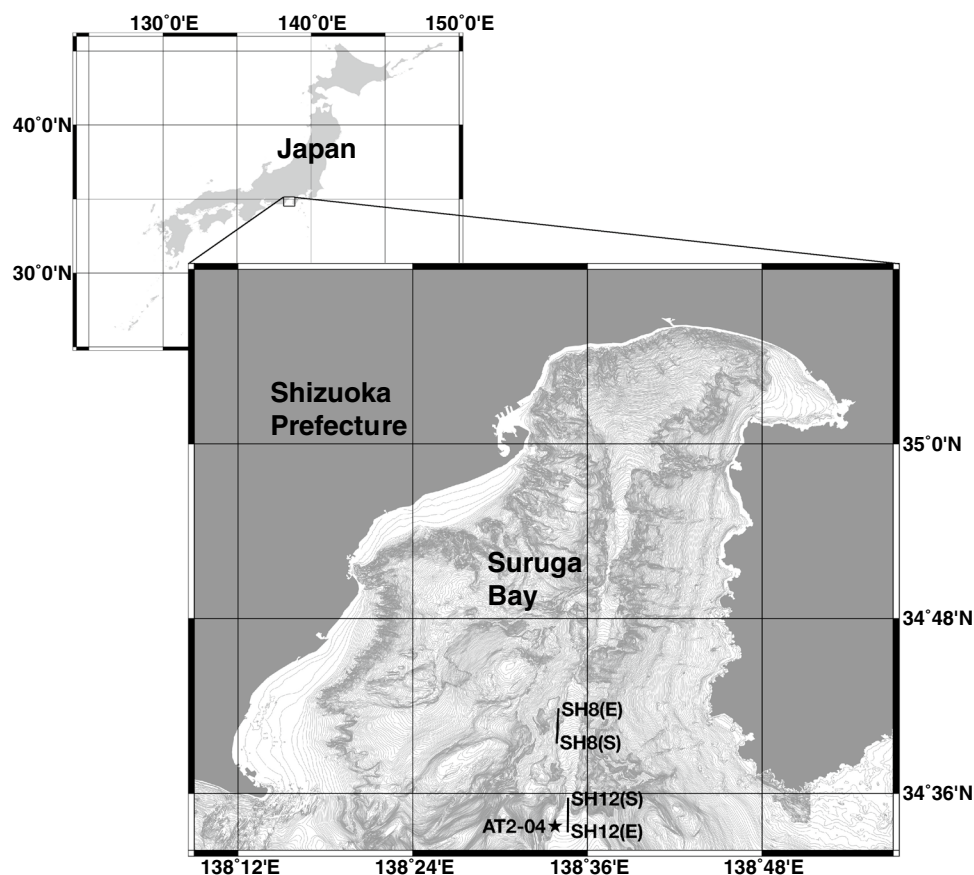


Figure 1. Research area and location of each longline and baited camera deployment. This map was created using QGIS software version 2.14.10 (<https://qgis.org/>) and bathymetric data M7001 supplied by the Japan Hydrographic Association (<https://www.jha.or.jp/en/jha/>). Solid line: longline tracks of SH8 and SH12; S and E represent the start and end locations of longlines, respectively. Solid star: deployment location of baited camera (AT2-04). This map is under copyright © 2018 Yoshihiro Fujiwara.

Sample ID	SH8-69	SH8-43	SH12-1	SH12-14
Sampling date	4th Feb. 2016	4th Feb. 2016	23rd Nov. 2016	23rd Nov. 2016
Longline no.	SH8	SH8	SH12	SH12
Depth (m)	2171	2179	2572	2551
Total length (cm)	138.0	122.0	125.0	132.0
Weight (kg)	22.6	14.8	19.0	24.9
Status	Holotype	Paratype 1	Paratype 2	Paratype 3
Catalogue number/deposited institution	1160053133/Japan Agency for Marine-Earth Science and Technology	KPM-NI 43548/Kanagawa Prefectural Museum of Natural History	NSMT-P 132616/National Museum of Nature and Science	CBM-ZF-0019048/Natural History Museum and Institute, Chiba

Table 1. Sampling dates and depths for the captured *Narctes shonanmaruae* specimens. Depth information was derived from the data logger records closest to each hooked fish.

fin base; pectoral fin base situated ventrolaterally on body, slightly closer to ventral margin than to lateral line; adipose fin absent; thick adipose layer between skin and muscle (“slippery” or “fatty tissue” layer).

Fins (Fig. 2b, Supplementary Figs. S4–S10): dorsal-fin rays, 14 in holotype and all the paratypes (including anterior three small rays); anterior four rays unbranched, 4th longest with 12 pterygiophores in holotype and 14 pterygiophores in paratype 1; anal-fin rays, 11 in holotype and paratype 2 and 3 (including anterior two small rays), 12 in paratype 1; anterior 3 rays unbranched, 4th longest with 11 pterygiophores in holotype and paratype 1; pectoral-fin rays, 11 in holotype and paratype 1, 12 in paratype 2, 13 in paratype 3; pelvic-fin rays, 9 plus a splint bone in holotype, 8 plus a splint bone in paratype 1, and 9 in paratypes 2 and 3 (splint bone unconfirmed due to no CT image); principal caudal-fin rays, 10 + 9 in holotype and paratype 1, and 10 upper and 9 lower precurrent rays in holotype and 11 upper and 9 lower in paratype 1.

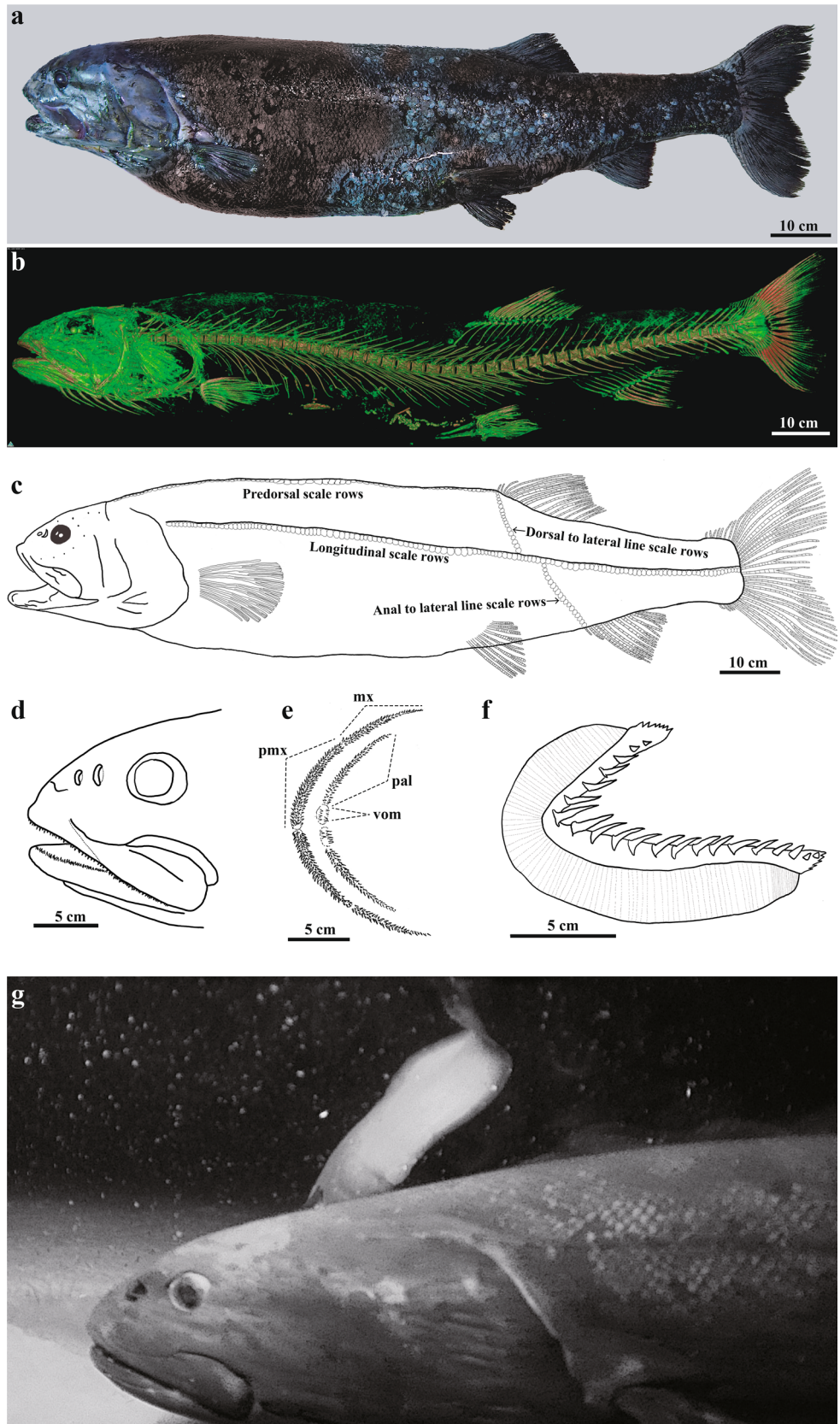


Figure 2. *Narcetes shonanmaruae*. (a), (b), (d), (e) holotype (SH8-69). (c) paratype 3 (SH12-14). (f) paratype 2 (SH12-1). (a) Lateral view. (b) Computed tomography image of the endoskeleton. (c) Lateral view. Scale rows indicated. Lateral line scales not shown. (d) Lateral view of head. (e) Tooth pattern of upper jaw. mx: maxillary, pal: platine, pmx: premaxillary, vom: vomer. (f) Gill raker. Right side of first arch. (g) In situ video grab of active swimming individual recorded using a baited camera.

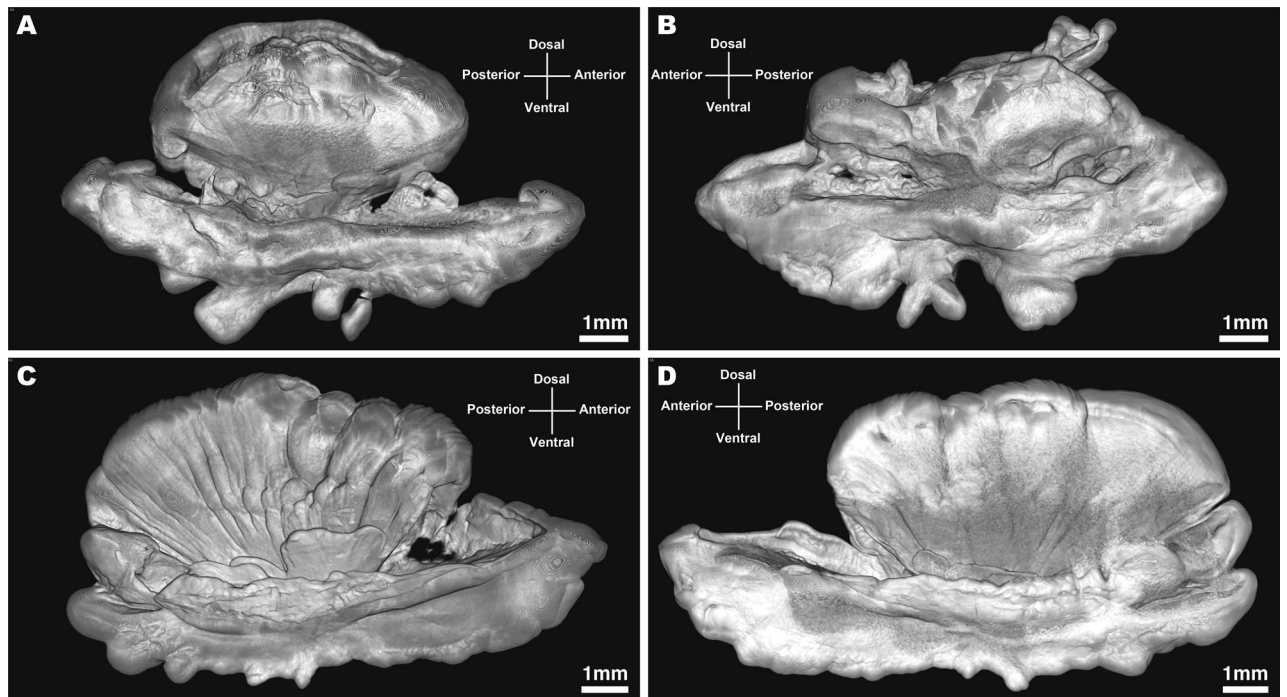


Figure 3. *Narcetes shonanmaruae*. Micro-computed tomography images of otoliths. (a) and (b) Holotype (SH8-69). (c) and (d) Paratype 1 (SH8-43). (a) and (c) Medial view of left otolith. (b) and (d) Medial view of right otolith. Scale bar: 1 mm.

Osteology (Figs. 1a,b, 2b,d,e, Supplementary Figs. S1–S4, S11, S16f): precaudal vertebrae, 28 and caudal vertebrae, 21 in holotype and paratype 1, amphicoelous (hour-glass shaped); neural and haemal spines prominent, all associated vertebral bones fully ossified; supraneurals present, situated above 10 most anterior precaudal vertebrae, seven supraneurals in holotype, five in paratype 1; epipleurals begin on 2nd vertebral centra; two epurals in holotype and paratype 1; posterior ural centra turned upwards; post-temporal, supracleithrum, and cleithrum forming almost right angles, thereby ‘squaring’ the head; presence of mesocoracoid and post-cleithrum indeterminate; circumorbital bones absent; opercle relatively small, slightly rounded, convex, except in front of pectoral base (concave); premaxillary broad with minute teeth, elongated, reaching halfway along the maxillary; maxillary almost double length of premaxillary, even broader, with minute teeth; two supramaxillae; dentary broad, covered with minute teeth in several rows.

Teeth (Fig. 2d,e, Supplementary Fig. S16f): many sharp teeth present on dentary, premaxillary, maxillary, vomer, and palatines, appear unordered, multiserial rows (teeth sockets present); number of teeth subject to allometric growth; tooth patches present on 5th ceratobranchial bone.

Scales (Figs. 1a, 2a,c, Supplementary Fig. S16a,b, Table 2): body scales relatively small, deciduous, cycloid and numerous, longitudinal scale rows 116–125, predorsal scale rows 73–88; isthmus sharply demarcated by absence of scales anteriorly, abruptly scaled posteriorly; skin on cleithrum without scales, demarcating head and angle between cleithrum and pectoral base; scales absent on nape; lateral line scales elongated, drawn into tube, expanded posteriorly, especially towards the tail region; skull and head region visibly naked, also sharply demarcated by purplish colour.

Others (Fig. 2a–d,f, Table 2, Supplementary Figs. S11, S16c–f): Lateral line straight, running along entire body; caudal fin slightly emarginate (Fig. 2a); eyes round, small relative to body size 2.9–3.5% SL; aphakic gap absent; paired nostrils, nasal cavities large, rosettes present immediately anterior to eyes, posterior largest, anterior round and less than half size of posterior; snout short (7.1–8.6% SL); seven branchiostegal rays; gill rakers (19–23) large, widely spaced, without teeth; small, slender pseudobranch filaments (12–14) present; photophores and swim bladder absent; pyloric caeca (9–13) extremely large; ovary developed in paratypes 2 and 3; ground body colour pigmentation purplish with scale pockets dark, appearing blackish/purplish (typical slickhead colouration); head, mouth, and gill cavities purplish/bluish.

Otoliths (Fig. 3, Supplementary Figs. S12–15): Otolith morphology ‘sailboat’ type¹⁵, variable within and between individuals, elongate anteroposteriorly, robust, outer face convex; sulcus deeply incised, not divided into ostium and cauda; crista superior absent, crista inferior present; dorsal part fan-shaped, including radial notches, dorsal rim variable, large hollow only present in holotype; ventral part ‘boat shaped’, including several lobes on ventral rim; rostrum present, gradually rising towards anterior tip; antirostrum present (rounded); posterior end relatively pointed.

Remarks. *Narcetes shonanmaruae* sp. nov. is similar to *N. erimelas* in anal fin position being entirely behind the dorsal fin. However, our species differs from all the other *Narcetes* species based on the following morphological

	<i>Narcetes shonanmaruae</i>					<i>Narcetes erimelas</i>			<i>Narcetes lloydi</i>	<i>Narcetes stomias</i>
	SH8-69	SH8-43	SH12-1	SH12-14	Species range	NSMT-P63883	<i>Bathytroctes alveatus</i> syntype	Species range	Species range	Species range
Standard length (SL) (cm)	121.0	104.0	111.5	117.5	104.0–121.0	21.8	~ 16.1	13.7–74.7	9.2–50.0	23.8–57.5
In % SL										
Predorsal length	61.2	60.6	61.4	62.1	60.6–62.1	64.7	–	61.8–65.7	58.9–66.7	61.5–66.4
Preanal length	76.3	73.4	77.9	78.3	73.4–78.3	80.3	–	76.4–81.4	67.9–78.1	67.6–74.8
Prepelvic length	59.9	58.5	60.3	64.9	58.5–64.9	61.5	(55.6)	61.2–63.2	49.9–58.8	50.5–58.8
Ventroanal length	16.8	15.8	20.4	18.5	15.8–20.4	15.6	–	14.4–18.3	–	–
Dorsal fin base length	12.2	12.2	12.1	12.6	12.1–12.6	14.3	–	13.1–16.9	13.4–19.4	13.4–17.6
Anal fin base length	7.6	7.3	7.7	8.1	7.3–8.1	9.4	–	8–10.8	10.0–13.8	9.2–12.8
Maximum body depth	13.5	18.3	22.9	23.8	13.5–23.8	17.9	(16.7)	15.2–23.8	15.7–22.7	14.3–22.1
Caudal peduncle depth	7.6	8.0	7.8	7.5	7.5–8.0	7.7	–	6.4–8.4	5.8–9.4	6.0–9.7
Caudal peduncle length	12.1	10.3	12.1	11.1	10.3–12.1	10.1	–	10.1–15.4	15.7–23.9	17.1–22.4
Postorbital width of head	9.8	9.0	8.9	8.6	8.6–9.8	9.5	–	9.5–12.5	8.6–13.4	8.9–11.3
Head length	24.4	27.4	24.7	24.5	24.4–27.4	36.3	34.2 (33.3)	28.9–38.8	26.6–36.6	26.8–32.1
Snout length	7.1	8.6	7.7	7.5	7.1–8.6	9.4	11.8 (10.0)	8.9–11.6	8.0–12.3	7.0–10.0
Orbit diameter	3.1	3.5	2.9	3.2	2.9–3.5	6.6	–	5.2–8.9	3.2–7.1	4.3–6.3
Interorbital distance	6.9	7.0	7.9	7.5	6.9–7.9	7.0	6.5 (6.7)	6.4–7.4	5.3–9.2	4.1–7.4
Upper jaw length	12.7	13.5	12.6	13.1	12.6–13.5	20.0	(> 16.7)	15.8–20.7	14.2–20.6	15.5–18.0
Lower jaw length	13.6	13.1	14.8	13.3	13.1–14.8	21.1	–	15.6–22.3	15.1–23.0	15.8–19.8
Dorsal-fin rays	14	14	14	14	14	15	15–16	15–17	17–22	17–21
Anal-fin rays	11	12	11	11	11–12	11	11	11–13	12?–18	14–18
Pectoral-fin rays	11	11	12	13	11–13	10	11	9–11	7–11	8–12
Pelvic fin rays	9	8	9	9	8–9	10	10(?)	8–10	8–10	7–10
Branchiostegal rays	7	7	7	7	7	??	–	7	8	8–9
Gill rakers on the first gill arch	6 + 16	5 + 14	6 + 15	6 + 17	[5, 6] + [14–17]	5 + 16 ^a	5 + 16	[5, 6] + [15, 16]	[5, 6] + [15–18]	[3–5] + [11–15]
Predorsal scale rows	77	88	79	73	73–88	37	–	37–40	27–37	42–60
Longitudinal scale rows	118	125	118	116	116–125	65 ^b	70	68–85	60–75	87–120
Dorsal to lateral line scale rows	18	19	19	18	18–19	10	7	7–12	8–11	9–12
Anal to lateral line scale rows	19	21	19	19	19–21	10	14?	10–14	9–12	9–14
Lateral line scale	60	54	58	62	54–62	NA	–	60	53–65	52–81
Pyloric caeca	9	13	11	13	9–13	–	–	10–14	8–16	6–12
Precaudal vertebrae (incl. skull-connecting vertebrae)	28	28	–	–	28	30	32 ^c	31–34	29–33	25–29
Caudal vertebrae (incl. vertebra articulated with parhypural)	21	21	–	–	21	22	19 ^c	19–23	23–25	20–23

Continued

	<i>Narcetes shonanmaruae</i>					<i>Narcetes erimelas</i>			<i>Narcetes lloydi</i>	<i>Narcetes stomias</i>
	SH8-69	SH8-43	SH12-1	SH12-14	Species range	NSMT-P63883	<i>Bathytroctes alveatus</i> syntype	Species range	Species range	Species range
Otolith (mm)										
Anteroposterior length										
Left	10.9	12.3	–	–	–	–	–	–	–	–
Right	11.5	13.0	–	–	–	–	–	–	–	–
Dorsoventral length										
Left	6.3	6.8	–	–	–	–	–	–	–	–
Right	7.1	6.8	–	–	–	–	–	–	–	–
Mediolateral length										
Left	3.0	2.7	–	–	–	–	–	–	–	–
Right	3.2	2.6	–	–	–	–	–	–	–	–
References	Present study	Present study	Present study	Present study	Present study	Present study	Sazonov ¹⁰ , Present study	Garman ⁸⁹ , Sazonov ¹⁰ , Present study	Sazonov ¹⁰	Sazonov ¹⁰

Table 2. Morphometric and meristic information on *Narcetes shonanmaruae* and relatives. –: Data not shown due to lack of measurements. ^aRight gill rakers counted due to malformation of left rakers. ^bRight scale rows counted due to sample condition. ^cCounted from syntype ID: MCZ 28477.

characters: length of dorsal fin base less than 13% SL; upper jaw length less than 14% SL; lower jaw length less than 15% SL; number of dorsal-fin rays less than 15; number of predorsal scale rows greater than 70; number of dorsal to lateral line scale rows greater than 16; number of anal to lateral line scale rows greater than 17.

Etymology. The species epithet *shonanmaruae* is a feminine noun in Latin, referring to the ship ‘*Shonan maru*’ from which the type materials were caught, honouring the vessel’s considerable contribution to deep-sea fish research in the area. The proposed Japanese vernacular name is ‘Yokozuna Iwashi’. This species belongs to the family Alepocephalidae, which is referred to as ‘Sekitori Iwashi’ in Japanese: ‘Sekitori’ meaning a sumo wrestler and ‘Iwashi’ meaning a sardine, thereby implying a massive sardine. The term ‘Yokozuna’ refers to the highest rank in sumo wrestling in Japan. Accordingly, we propose the name ‘Yokozuna Iwashi’ as being indicative of the large body size and the high trophic position of the newly described species. English vernacular name: Yokozuna Slickhead.

Distribution. Currently only known from Suruga Bay at depths deeper than 2100 m.

Phylogenetic placement of *Narcetes shonanmaruae*. Mitogenomic DNA sequences for the *N. shonanmaruae* holotype (SH8-69) and paratype 1 (SH8-43), in addition to those for three species of *Conocara* and *Talismaania antillarum*, were determined in the present study and deposited in nucleotide sequence databases under the accession numbers shown in Supplementary Table S1. Each translated amino acid sequence was aligned with homologues from 73 other teleost species (75 operational taxonomic units, OTUs, in total, accession numbers shown in Supplementary Table S1). The evolutionary models selected for the maximum likelihood (ML) analysis of each amino acid sequence of 13 mitochondrial protein-coding genes are shown in Supplementary Table S2. The aligned positions of the 13 proteins from each species combined had a total length of 3790 amino acids.

The phylogenetic position of *N. shonanmaruae* determined from our ML analysis was distinct from that of all other alepocephalid fish (Fig. 4). The phylogenetic analyses showed that *N. shonanmaruae* is a sister species of *Narcetes erimelas* known from the Pacific, Eastern Central Atlantic, and Indian Ocean at depths of between 1300 and 2740 m^{10,13} (Fig. 4). The genetic distances between the *COI* gene sequences of *N. shonanmaruae* and *Narcetes erimelas* are 0.017–0.018, which are greater than the intraspecific values in *N. shonanmaruae* (0.000–0.002). The bootstrap value in the ML analysis (94%) indicated the monophyly of this clade. The monophyly of the order Alepocephaliformes was supported by a bootstrap value of 100%. The family Alepocephalidae was not monophyletic due to the phylogenetic position of *Bathylaco nigricans* that fell into a single clade with four species from the family Platytroutidae, and the bootstrap value did not strongly support monophyly (Fig. 4).

Stomach content analysis. Stomach contents were analysed from two individuals of *N. shonanmaruae* (SH8-69 and SH8-43), both of which contained chyme. In addition, the stomach of the holotype (SH8-69) contained a pair of fish otoliths (~5 mm in diameter). However, due to the advanced state of degradation, it was not possible to identify the species of prey fish from these otoliths.

DNA barcoding targeting prey mitochondrial *COI* genes was performed using chyme collected from the holotype. After removal of low-quality reads, chimeric sequences, and singletons from all detected reads, ~200,000 reads were obtained and were clustered in three different OTUs (Supplementary Table S3). OTU1 (85%

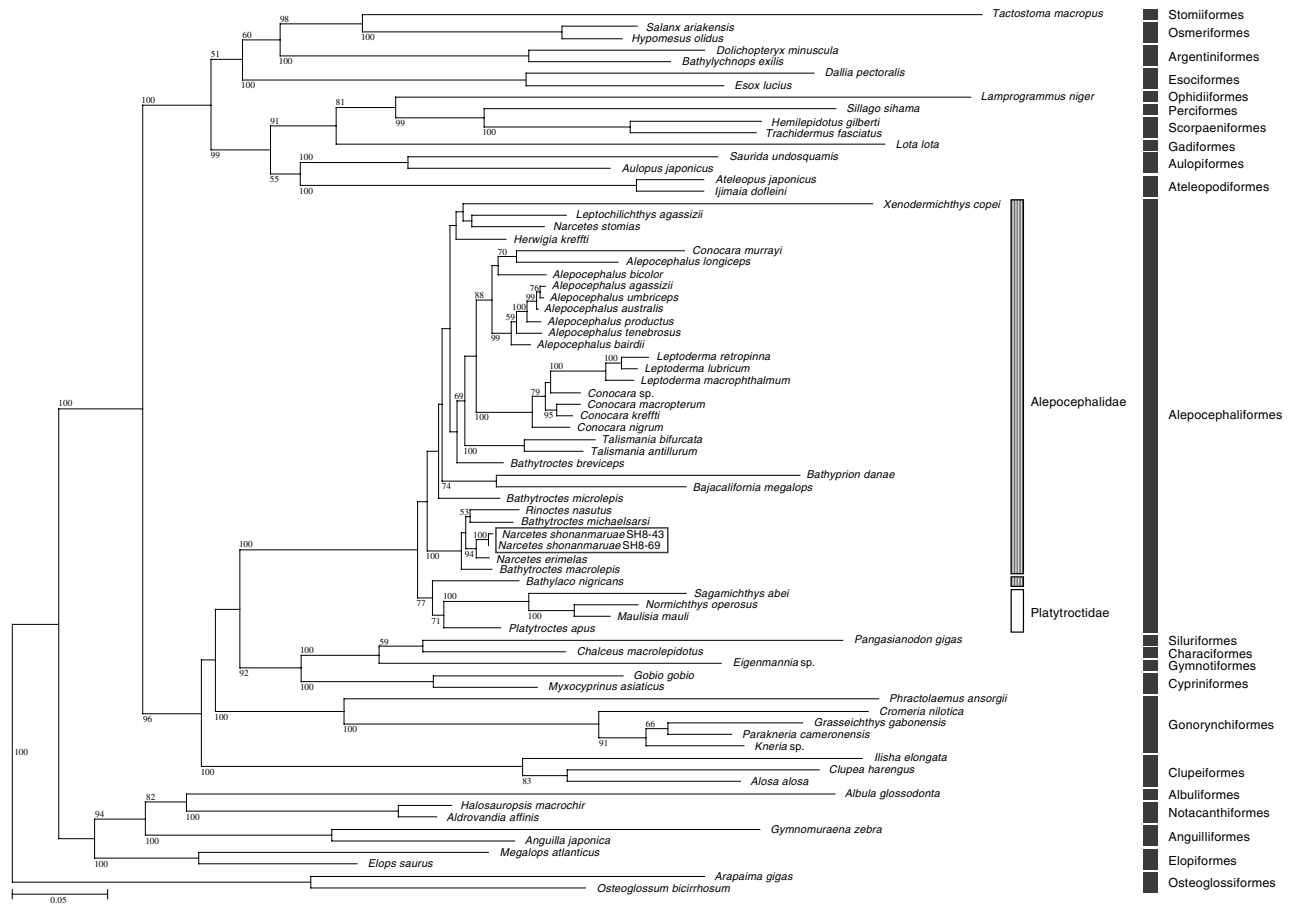


Figure 4. Phylogenetic placement of *Narcetes shonanmaruae* based on amino acid sequences from 13 protein-coding genes of the mitogenome. A maximum likelihood (ML) tree is shown. Scale bar represents 0.05 nucleotide substitutions per sequence position. Bootstrap values are shown for each branch. *Narcetes shonanmaruae* is highlighted.

appearance in the total reads) was derived from *N. shonanmaruae* despite the use of blocking PCR primers designed to reduce amplification of the host DNA. OTU2 (9% appearance in the total reads) showed highest identity (91%) with the mitochondrial *COI* gene of the genus *Bassozetus* in the family Ophidiidae. OTU3 (6% appearance in the total reads) showed highest identity (88%) with the fungal genus *Cortinarius* (Agaricomycetes; Agaricomycetidae).

Compound-specific isotope analysis of amino acids. The nitrogen isotopic composition of amino acids and the trophic positions (TPs) estimated from the values of glutamic acid and phenylalanine are shown in Table 3 and Fig. 5. The estimated TPs of the two examined *N. shonanmaruae* individuals were both 4.9, which was the highest among the predatory fishes examined in this study. The nitrogen isotopic compositions of phenylalanine from *N. shonanmaruae* (#15 and #16) (-3.0‰ and 0.1‰ , respectively) were slightly lower than those of the other fish species examined (#1–14) ($+3.9\text{‰}$, $SD = 1.5$, $n = 14$) (Fig. 5).

In situ observation of *Narcetes shonanmaruae* using a baited camera. Four baited camera casts were conducted at depths greater than 2000 m in Suruga Bay (~16 h of video footage in total), and a single individual of *N. shonanmaruae* was observed in the bay mouth on 26th November 2016 during cast no. AT2-04 at a depth of 2572 m (Figs. 1, 2g, Supplementary Table S4, Supplementary Video S1). A 12-s sequence of high-definition video footage showed that this *N. shonanmaruae* individual swam into the video frame from the right side and then changed direction towards a position out of view of the camera lens (Supplementary Video S1). The fish vigorously beat its tail fin when veering. Its total length estimated from the video image was more than 100 cm. Individuals of the pudgy cusk-eel *Spectrunculus grandis* and lithodid crab *Paralomis* sp. were also observed in the video recordings, as shown in Supplementary Video S1.

Discussion

In this paper, we describe a novel slickhead fish species, which was collected from deep-water sites within Suruga Bay, Japan. To the best of our knowledge, this species is the largest among species in the family Alepocephalidae, and its trophic position is one of the highest among marine organisms reported globally to date^{13,16,17}.

No	Species	Location	Habitat	Total Length (cm)	Weight (kg)	$\delta^{15}\text{N}$		
						Glu	Phe	$\text{TP}_{\text{Glu/Phe}}$
1	<i>Chlamydoselachus anguineus</i>	Suruga Bay	Bathydemersal	NA	NA	27.3	3.8	3.7
2	<i>Chlamydoselachus anguineus</i>	Suruga Bay	Bathydemersal	156.0	NA	28.1	3.6	3.8
3	<i>Odontaspis ferox</i>	Suruga Bay	Benthopelagic	162.4	NA	27.7	3.0	3.8
4	<i>Odontaspis ferox</i>	Suruga Bay	Benthopelagic	124.3	9.8	28.0	3.1	3.8
5	<i>Somniosus pacificus</i>	Suruga Bay	Benthopelagic	178.6	48.4	30.0	4.4	3.9
6	<i>Mitsukurina owstoni</i>	Suruga Bay	Bathydemersal	223.6	35.9	27.4	1.5	4.0
7	<i>Heptranchias perlo</i>	Suruga Bay	Bathydemersal	115.5	NA	29.6	3.5	4.0
8	<i>Mitsukurina owstoni</i>	Suruga Bay	Bathydemersal	212.0	23.1	29.8	3.6	4.0
9	<i>Heptranchias perlo</i>	Suruga Bay	Bathydemersal	NA	NA	31.9	4.4	4.2
10	<i>Hexanchus griseus</i>	Suruga Bay	Bathydemersal	271.6	119.1	32.9	5.3	4.2
11	<i>Centroscymnus owstonii</i>	Suruga Bay	Bathydemersal	78.6	2.6	30.9	2.4	4.3
12	<i>Hexanchus griseus</i>	Suruga Bay	Bathydemersal	NA	NA	33.1	4.6	4.3
13	<i>Pseudotriakis microdon</i>	Suruga Bay	Bathydemersal	208.4	43.0	37.1	7.8	4.4
14	<i>Centroscymnus owstonii</i>	Suruga Bay	Bathydemersal	112.2	NA	33.5	3.5	4.5
15	<i>Narctes shonanmaruae</i> SH8-43	Suruga Bay	Benthopelagic	122.0	14.8	29.9	-3.0	4.9
16	<i>Narctes shonanmaruae</i> SH8-69	Suruga Bay	Benthopelagic	138.0	22.6	33.3	0.1	4.9

Table 3. The trophic position of fishes examined in this study. Positions were calculated using the nitrogen isotopic compositions of glutamic acid and phenylalanine using the following equation: $\text{TP}_{\text{Glu/Phe}} = (\delta^{15}\text{N}_{\text{Glu}} - \delta^{15}\text{N}_{\text{Phe}} - 3.4)/7.6 + 1$.

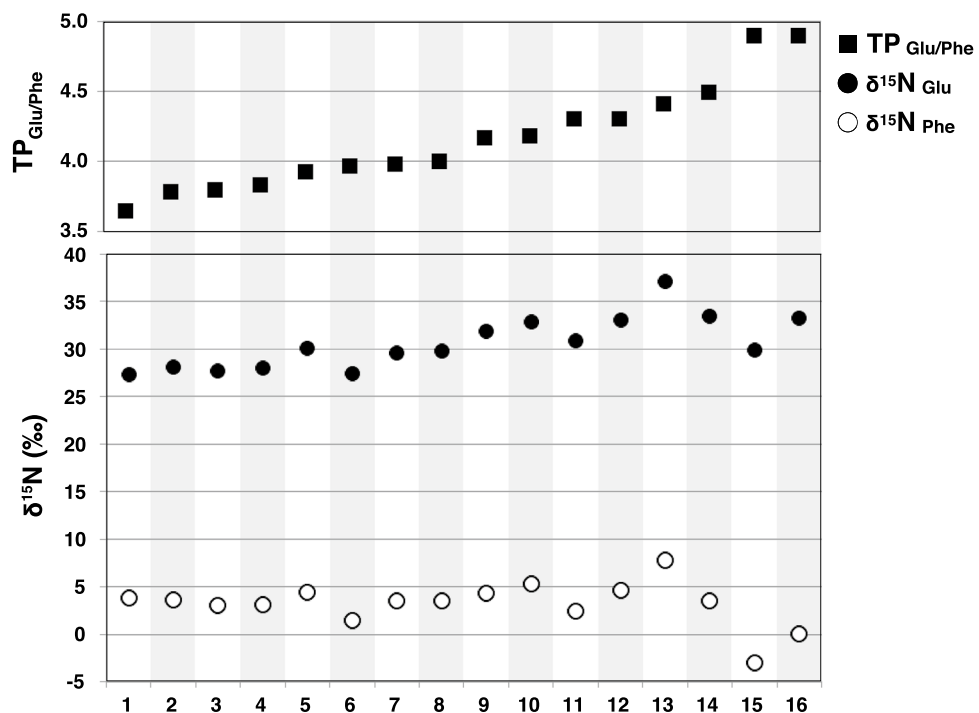


Figure 5. Nitrogen isotopic compositions and trophic positions of deep-sea fish collected in Suruga Bay. Solid circles: nitrogen isotopic compositions of glutamic acid, open circles: nitrogen isotopic compositions of phenylalanine, solid squares: trophic positions (TP) estimated using values of the nitrogen isotopic compositions of glutamic acid and phenylalanine ($\text{TP}_{\text{Glu/Phe}}$). Values of organisms were based on the primary production of phytoplankton. $\text{TP}_{\text{Glu/Phe}}$ was calculated using Eq. (1) with a β value of -3.4‰ . The numbers shown beneath the graph are the sample numbers indicated in Table 3.

Maximum standard lengths (SL) of 77 species from the family are presented in FishBase and a previous study^{10,13,16} (summarized in Supplementary Table S5). A frequency distribution of SL in Alepocephalidae clearly shows that *N. shonanmaruae* and two other slickheads (*Alepocephalus bairdii* and *A. agassizii*) are much larger compared to other species in the family, exceeding 100 cm in SL (Supplementary Fig. S17). The length range with highest frequency in SL is 20–40 cm, and the average maximum SL is 35.3 cm ($n = 78$, $SD = 21.5$, including the present species), which demonstrate the large size of *N. shonanmaruae*.

Deep-sea gigantism, which was first described for a plaice species *Pleuronectes platessa* showing a size increase with depth¹⁸, has previously been reported in various marine taxa, e.g. the giant squid *Architeuthis dux*, the giant deep-sea isopod *Bathynomus giganteus*, the Japanese spider crab *Macrocheira kaempferi*, the bluntnose sixgill shark *Hexanchus griseus*, and the oarfish *Regalecus glesne*¹⁹. Although there is currently no generally accepted explanation for the deep-sea gigantism observed in fishes, it has been proposed that, in crustaceans, this phenomenon is a consequence of larger cell size that develops in response to lower temperatures²⁰, as has also been proposed for other groups²¹. In crustaceans, deep-sea gigantism may also in part reflect decreases in temperature leading to a longer lifespan and thus larger sizes for species with indeterminate growth²⁰. Among fish taxa, scavenging species, identified as those that regularly appear at baited cameras, increase in size with depth, whereas non-scavenging species decrease in size over the same depth range^{22,23}. The gigantism of deep-sea fish could be interpreted in terms of a response to differences in the characteristics of food supply by the two groups²². Scavenging species depend on large, randomly distributed packages of carrion falling from the shallower waters, and a larger body size permits greater swimming abilities and endurance, thereby allowing the fish to move efficiently between occasional feeding events in the deep sea²³. Trophic level and body size are also believed to be positively correlated across all the species examined, and morphological constraints associated with gape limitation may play a prominent role in determining body size²⁴. Deep-sea alepocephaliform fishes are highly diverse, particularly within the family Alepocephalidae (slickheads), which consists of more than 90 species recorded globally^{25–27}. Slickheads have been suggested to be important consumers of gelatinous zooplankton^{28–30}, and generally show lower trophic positions than that of other fishes living in the same environments^{31,32}. Thus, the feeding ecology and the trophic level of *N. shonanmaruae* would appear to be unique in this family. The scavenging ability (as implied by capture using a longline) and broad gape of *N. shonanmaruae* (Supplementary Fig. S16f) might be correlated with its colossal body size and relatively high trophic position.

The estimated trophic positions (TP = 4.9) of the two individuals for which stomach contents were analysed were the highest among the predators examined in the present study and are relatively high compared with the values obtained in previous studies^{17,33–36}. The bluntnose sixgill shark *H. griseus* is known as an apex predator/scavenger in the deep sea^{37–39}, whereas the false catshark *Pseudotriakis microdon* is a large predatory shark that reaches 3 m in length and feeds on a wide variety of prey, including teleost and chondrichthyan fishes, cephalopods, and marine mammals⁴⁰. The trophic positions determined for *H. griseus* (4.2 and 4.3) and *P. microdon* (4.3) in the present study are all lower than that of *N. shonanmaruae*. Since trophic positions estimated from stable isotope analysis provide long-term dietary information^{41,42}, these results indicate that *N. shonanmaruae* commonly feeds on high-trophic prey (TP = ca. 4). Nielsen et al.¹⁷ compiled amino acid stable nitrogen isotope ratios from 359 marine species covering four trophic levels (primary producer, herbivore, omnivore, and carnivore) from the literature. We calculated all the TPs in this previous study using Eq. (1) shown in the Methods section with β values of -3.4‰ . The highest TP among all taxa listed was observed in an unidentified dogfish shark *Squalus* sp. (TP = 4.8), and the highest in a teleost was observed in a moray eel *Gymnothorax kidako* (TP = 4.7). Both species are aggressive predators, and the TP values are comparable to that of *N. shonanmaruae*. Although further information is needed on the trophic positions of other species from the deepest waters of Suruga Bay in order to clarify the relative position of *N. shonanmaruae* in the bathyal ecosystem, there is little doubt regarding the relatively high trophic position of this slickhead in marine environments.

The nitrogen isotopic compositions of phenylalanine from *N. shonanmaruae* were slightly lower than those of the other fish species examined (Fig. 5). Such differences are within intra/inter-species variations collected from same regions. Intra-species variations of phenylalanine $\delta^{15}\text{N}$ values were reported from a largescale blackfish *Girella punctata* collected sympatrically in Sagami Bay, Japan (the values ranging from 3.7 to 8.7), but the TPs were nearly consistent (TP ranging from 2.7 to 3.1) because the nitrogen isotopic compositions of glutamic acid fluctuated according to those of phenylalanine³⁶. The phenylalanine $\delta^{15}\text{N}$ values were also variable between planktonic/pelagic taxa collected at a same site 100 km north of the island of Oahu in the North Pacific Subtropical Gyre⁴³, ranging from -4.8 to 7.5 , which is comparable to the values found in the results of the present study (Fig. 5).

Both morphological analyses and DNA barcoding of stomach contents showed *N. shonanmaruae* to be piscivorous in its feeding habits. In this regard, although a pair of fish otoliths was found in the stomach of the holotype, prey species identification was not possible due to the severe degradation of these otoliths. Even though the stomachs of both analysed individuals were almost empty, small amounts of chyme were detected. Such a paucity of stomach contents is common among deep-sea fish that tend to regurgitate their stomach contents upon being landed⁴⁴. DNA meta-barcoding of the stomach chyme also supported a piscivorous habit. A sequence similarity search for sequences amplified from the chyme indicated the prey item to be an ophidiid fish (Family Ophidiidae), which comprise a dominant group of deep-sea demersal fishes containing 218 known species^{45,46}. This result is consistent with a predatory lifestyle. *N. shonanmaruae* possesses large, widely spaced gill rakers (Fig. 2f, Supplementary Fig. S16c). In general, gill rakers play the role of entrapment structures to retain planktonic prey from a volume of engulfed water and are thus common in planktivorous filter feeding fish^{47,48}. Increasing the number of gill rakers enhances crossflow filtering and the closely spaced gill rakers also limit the escape possibilities of small prey. However, a dense gill raker apparatus is more likely to become clogged by sediments than sparser gill rakers, and foraging in the muddy bottom of the profundal zone most likely requires other gill raker adaptations. Accordingly, a high number of long gill rakers is common in planktivorous fish species, whereas

benthic species usually display a lower number of shorter gill rakers^{49–52}. The rakers of *N. shonanmaruae* seem to be too sparse to support filter feeding, which is inconsistent with a planktivorous feeding habit.

Cannibalism of this slickhead might be possible, because the most dominant OTU from DNA meta-barcoding of the stomach chyme was the sequences of *N. shonanmaruae* even though a blocking primer against the *N. shonanmaruae* sequence was applied. However, several previous studies showed amplification of host sequences from stomach contents in spite of using specific blocking primers against the host^{53,54}. In addition, there is no record of smaller individuals of this slickhead at any depths in Suruga Bay (Y. F., unpublished data), which implies difficulty in smaller *N. shonanmaruae* individuals being the staple diet for adults. Somewhat incongruously, OTU3 showed high homology with several species of Agaricomycetes (Fungi) and Oomycetes (Stramenopiles). As these are not considered to form part of the *N. shonanmaruae* diet, it is assumed that they could be experimental contaminants of terrestrial origin^{55,56}. Alternatively, they might be unknown parasitic organisms present in the digestive apparatus of slickheads or environmental DNA included in the stomach sample.

Our video observations revealed that *N. shonanmaruae* is an active swimmer (Supplementary Video S1). In the same video sequence, we observed the most dominant fishes living at the depth (*Spectrunculus grandis*, *Simenchelys parasitica*, and *Coryphaenoides acrolepis*), which are taeniform or anguilliform species that do not move rapidly^{57,58}. In contrast, the newly discovered slickhead—being fusiform and possessing a narrowed but robust caudal peduncle with a relatively large emarginate caudal fin—was observed veering vigorously with a single tail stroke and rapidly disappearing from the video frame. Such a body plan and swimming behaviour are consistent with the stomach contents (i.e. fish) and a high trophic position, all indicating that this slickhead is probably a top predator in the deepest part of Suruga Bay.

Each year, many new species of fish are discovered, most of which are relatively small^{13,59}. In contrast, discoveries of large bony fishes from marine environments have been relatively rare in recent years. Since the 1800s, Suruga Bay has been one of the most studied bays in Japan^{4–6}, and has yielded many marine organisms described as new species^{60–62}. Deep-sea fishing, including that using longlines and bottom trawls, continues to be practiced in Suruga Bay, and therefore the deep-sea fauna inhabiting this bay is relatively well documented^{7–9}. The discovery of a colossal slickhead from this bay was thus completely unexpected. In the present study, we conducted two longline searches at depths greater than 2171 m during two separate cruises and collected two individuals from each line. This high encounter probability might be due to a combination of the research method used and depth searched. Longline fishing is generally conducted at shallower depths (shallower than 1000 m in Suruga Bay) because of the difficulty of line control and limited profitable catches. Scientific trawls and dredges have sometimes been conducted at greater depths, although it is difficult to collect large, fast swimmers. In this regard, obvious differences in size and species selectivity of longlines and trawl nets have been reported⁶³, and it is highly likely that further longline-based surveys in deep waters will reveal the actual diversity of deep-sea predators, not only in Suruga Bay but also in many marine environments worldwide.

Top predators play an important role in the maintenance of species diversity and of ecosystem functions^{64–67}. The extinction and reintroduction of gray wolves in Yellowstone National Park is an example of the drastic change in a population of top predators affecting the entire ecosystem⁶⁸. Similar instances are too frequent to enumerate not only in terrestrial but also in marine ecosystems^{65,69,70}. “Fishing down the food web”⁷¹ occurs even in the deep sea that is the largest habitat for life on the Earth. Trophic positions of catches from deep sea are quite high (from 3.5 to 4.5 predominantly, estimated using FishBase), and some fish resources have already been depleted due to over fishing⁷². Oceanic warming, acidification, and deoxygenation are occurring even in the deep sea¹, which is assumed to initially affect large, predatory consumers. If the deep-sea ecosystems are severely damaged through the trophic cascade like that in Yellowstone, its influence on the global environment is immeasurable. As an initial step, there is an urgent need to conduct a broad and precise census of predators in the deep oceans to facilitate protection of natural resources of the planet and human livelihoods.

Methods

Bottom longline. In 2016, two research cruises were conducted in January–February (SH16-01) and in November–December (SH16-02) in Suruga Bay using the training vessel *Shonan maru* belonging to the Kanagawa Prefectural Marine Science High School. Two research longlines, SH8 and SH12, were deployed on the bottom of the Suruga Trough at the mouth of the bay on 3rd and 4th February and 22nd and 23rd November 2016, respectively (Fig. 1). The coordinates and depths of the surveyed sites are shown in Supplementary Table S4. Both longlines were left overnight on the deep-sea floor, and then retrieved onboard.

The longlines were composed of a 4-km main line (5 mm in diameter, polyester), 400 hooks with 5-m branch lines through the main line, two 10-kg lead sinkers, and a radio buoy at each end of the main line. A half or one-third portion of mackerel was impaled on each hook as bait. Three miniature salinity, temperature, and depth loggers (DST-CTD; Star-Oddi, Garðabær, Iceland) were attached to the start, mid, and end points of the main lines. This study was conducted in accordance with the Guidelines for Proper Conduct of Animal Experiments published by the Science Council of Japan, and the guidelines for fish experiments published by the Nature Conservation Committee of the Ichthyological Society of Japan. All the field experiments were approved by the Research Safety Committee of the Japan Agency for Marine-Earth Science and Technology.

Morphological observations and X-ray tomography scanning. The total body lengths and weights of the four alepocephaliform fish caught using longlines were measured. All the individuals were immediately frozen onboard. After completion of the cruises, additional observations and detailed measurements of individuals were performed in the laboratory. Morphological characters of this alepocephaliform fish were compared to those in previous studies^{10,11,73–77}. X-ray CT scanning of two individuals (holotype and paratype 1) was conducted for observations of osteological characteristics using a Discovery 750 HD CT scanner (GE Health-

care, Waukesha, WI, USA) under the following conditions: tube voltage, 120 kV; tube current, Auto mA; section thickness, 0.625 mm; rotation time, 1.0 s; and pitch, 0.984:1. Taxonomic keys were referred from previous studies⁷⁴.

Microfocus X-ray CT morphological analysis of otoliths. Morphological analyses of otoliths from two individuals were conducted using a microfocus X-ray CT scanner (ScanXmate–D160TSS105; Comscantecno Co. Ltd., Kanagawa, Japan). This system applies X-rays to a sampling stage, which rotates 360 degrees, with a high-resolution setting (X-ray focus spot diameter of 0.8 μm , X-ray tube voltage of 45 kV, detector array size of 1024 \times 1024, 1200 projections/360°, two-times averaging, sequential imaging, 2.0 s/projection). Spatial resolution of scanning was changed from 7 to 15 μm , depending on the size of otoliths. Reconstruction of three-dimensional (3D) tomographic images was performed with ConeCTexpress^(R) software (Comscantecno Co. Ltd., Kanagawa, Japan) using the convolution back-projection method. In order to avoid artefacts associated with 3D image reconstruction, noise-cancelling and ring-artefact filters were applied. Calculations of lengths, volumes, and other morphological properties were performed using Molcer Plus imaging software (White Rabbit Corp. Inc., Tokyo, Japan).

DNA sequencing. Total DNA was extracted from the muscle tissue of *N. shonanmaruae* specimens using a DNeasy Tissue and Blood Kit (QIAGEN Japan, Tokyo, Japan). Tissue samples of four other slickhead species were provided by Academia Sinica, Taiwan (three *Conocara* species), and Tokai University, Japan (*Talismania antillarum*), and used for DNA extraction. The sample IDs of these species are shown in Supplementary Table S1. Extracted DNA was used as a template for PCR amplification to amplify the mitogenome. Two universal primer sets for the mitochondrial 16S rRNA gene⁷⁸ and the COI gene⁷⁹ were used for PCR (Supplementary Table S6). In addition, three degenerate primer sets were designed for ATPase F0 subunit 6 (*ATP6*), NADH dehydrogenase subunit 4 (*ND4*), and cytochrome *b* (*cytb*) genes (Supplementary Table S6), based on the sequences from several alepocephalid species deposited in nucleotide sequence databases. After PCR amplification and partial sequencing of the genes, additional primers specific to *N. shonanmaruae* were designed to amplify five long fragments from the mitogenome (Supplementary Table S6). Specific primers used for sequencing of the mitogenomes of the four additional slickheads were designed in the same manner. PCR was performed using an Ex Taq Kit (TaKaRa, Kyoto, Japan). All the PCR products were purified using a Wizard SV gel and PCR purification Kit (Promega KK, Tokyo, Japan). The purified fragments were used for sequencing reactions using a Big Dye Terminator v3.1 Cycle Sequencing Kit (Applied Biosystems, Foster City, CA, USA). Sequencing was performed using an ABI PRISM 3130xl Genetic Analyzer (Applied Biosystems Japan Ltd., Tokyo, Japan). After sequencing, assembling and ambiguity editing of each sequence were conducted using CodonCode Aligner software (CodonCode Corporation, Dedham, MA, USA) to reconstruct whole mitogenome sequences.

Phylogenetic analysis. Seventy-five OTUs (six obtained in the present study and the remainder from nucleotide sequence databases) were used for phylogenetic analysis, among which those of two Osteoglossiformes species (*Arapaima gigas* and *Osteoglossum bicirrhosum*) were used as an operational outgroup (Supplementary Table S1). All the 13 protein-coding genes (*ND1*, *ND2*, *COI*, *COII*, *ATP8*, *ATP6*, *COIII*, *ND3*, *ND4L*, *ND4*, *ND5*, *ND6*, and *cytb*) in the mitogenome were used for phylogenetic analysis. The predicted amino acid sequences of the 13 protein-coding genes were independently aligned using MAFFT v7.164b⁸⁰ with auto parameters, followed by automatic editing of the resulting alignments using the GBLOCKS program^{81,82}. An appropriate evolutionary model for each gene alignment was then selected for maximum likelihood (ML) analysis using Aminosan software⁸³, based on Akaike Information Criteria (Supplementary Table S2). Amino acid sequence alignments from each gene were concatenated (3790 amino acids from 75 OTUs in total). ML analysis using the concatenated alignment of fish mitochondrial genes was performed using RAxML version 8.2.10⁸⁴, with appropriate evolutionary models selected. ML bootstrap probability analysis was performed using the same software with 100 resamplings.

Dietary analyses. The abdominal cavities of two *N. shonanmaruae* individuals (SH8-69 and SH8-43) were dissected prior to formalin fixation. Each stomach was excised, and the entire stomach contents were retrieved. The contents were visually examined, and prey items were selected from the digested materials. The chyme from one individual was used for DNA meta-barcoding analysis targeting residual prey DNA. DNA extraction, library preparation, and high-throughput sequencing were performed by Bioengineering Lab. Co., Ltd. (Kanagawa, Japan) as follows. Approximately 20 g of stomach chyme was freeze-dried and completely homogenized. DNA was isolated from the homogenized material using an ISOSPIN Blood & Plasmid Kit (Nippon Gene, Tokyo, Japan). Short fragments of *COI* genes were amplified using modified metazoan universal primer sets⁸⁵, incorporating forward and reverse adapter sequences, i.e. ACACTCTTCCCTACACGACGCTCTTCCGATCTGGWACWGGWTGAACWGTWTAYCCYCC and GTGACTGGAGTTCAGACGTGTGCTCTTCCGATCTTAHACTTCNGGGTGKCCRAARAATCA. In this procedure, a set of blocking primers was used to prevent amplification of the *COI* gene from the predatory (host) fish, as described previously⁸⁶. Using the PCR products, paired-end sequence libraries were constructed according to the tailed PCR method, and these libraries were sequenced using Illumina MiSeq (Illumina, San Diego, CA, USA) under 2 \times 250 bp conditions. After removing low-quality reads, OTUs were constructed. A homology search of each OTU was subsequently performed to identify prey animals from the stomach.

Nitrogen isotope analysis of individual amino acids. The extraction and derivatization of amino acids and nitrogen isotope analyses of specific amino acids were conducted according to the methods described

in previous studies^{35,87}. Each sample was hydrolysed with 12 M HCl at 110 °C for 12 h. The hydrolysate was filtered to remove any precipitate using Pall Nanosep MF Centrifugal Devices containing a GHP Membrane (Pall, Port Washington, NY, USA), and then washed with *n*-hexane/dichloromethane (3:2, v/v) to remove hydrophobic constituents. The derivatization of amino acids was performed sequentially using thionyl chloride/2-propanol (1:4, v/v) at 110 °C for 2 h and pivaloyl chloride/dichloromethane (1:4, v/v) at 110 °C for 2 h. The Pv/iPr derivatives of the amino acids were extracted with *n*-hexane/dichloromethane (3:2, v/v). The nitrogen isotopic composition of the individual amino acids was determined by GC/C/IRMS using an Agilent Technologies 6890 N gas chromatograph (Agilent Technologies, Santa Clara, CA, USA) coupled to a Thermo Fisher Scientific Delta^{plus}XP mass spectrometer (Thermo Finnigan, Bremen, Germany) with a GC-C/TC III interface^{35,87}. The isotopic composition was reported as the $\delta^{15}\text{N}$ notation relative to atmospheric N_2 (AIR). The analytical error was better than $\pm 0.5\%$. The TP of samples ($\text{TP}_{\text{Glu/Phe}}$) was calculated from the $\delta^{15}\text{N}$ values of glutamic acid ($\delta^{15}\text{N}_{\text{Glu}}$) and phenylalanine ($\delta^{15}\text{N}_{\text{Phe}}$) using Eq. (1) with β values of -3.4% .

$$\text{TP}_{\text{Glu/Phe}} = [(\delta^{15}\text{N}_{\text{Glu}} - \delta^{15}\text{N}_{\text{Phe}} + \beta)/7.6] + 1 \quad (1)$$

Baited camera observations. Baited camera observations were conducted on 26th November 2016 at depths greater than 2000 m in the mouth of Suruga Bay (Fig. 1, Supplementary Table S4). The camera system consisted of a high-definition video camera (KCN-EV7520SDI; Totsu Sangyo, Tokyo, Japan), an HD-SDI recorder (HDS-1601; Totsu Sangyo), an LED light array composed of 20 red LEDs (OSR5XNE3C1E; OptoSupply, Hong Kong) fixed with an epoxy resin⁸⁸, an acoustic releaser (STD-301; Kaiyo Denshi, Saitama, Japan), a sinker-releasing unit (PJ-0001; Pearl Giken, Chiba, Japan), a DST-CTD logger (Star-Oddi), a current profiler (Zpulse Doppler current sensor 4930; Aanderaa, Bergen, Norway), and two batteries (9200WP-L; Daiwa, Tokyo, Japan). The camera system was deployed from *Shonan maru* in free-fall mode. A 30-kg ballast was released by the acoustic releaser according to the release command from the ship. Video recording was started 30 min before landing and yielded a 5-h video footage. All the data, including videos and current profiles, were recovered when the system was retrieved onboard.

Comparative material (X-rays available for all specimens, upon request).

Narctes erimelas: ZMUB uncat. (Mar-eco 3948), 237.2 mm SL, ZMUB uncat. (Mar-eco 3691), 271.0 mm SL.

Narctes erimelas: NSMT-P63883, 218.0 mm SL.

Narctes erimelas (originally described as *Bathytroctes alveatus*): MCZ 28477, 152.2 mm SL (measured from X-ray image).

Bathytroctes michaelsarsi: ZMUB 16003 (Mar-eco 7297), 401.5 mm SL.

Bathytroctes macrolepis: ZMUB 15996 (Mar-eco 11860-1), 247 mm SL; ZMUB uncat. (Mar-eco 11860-2), 228.0 mm SL; ZMUB uncat. (Mar-eco 11860-3), 227.5 mm SL; ZMUB uncat. (Mar-eco 3403), 330 mm SL; ZMUB uncat. (Mar-eco 2711), 271 mm SL; ZMUB 15995 (Mar-eco 3904), 185.2 mm SL.

Rinoctes nasutus: ZMUB 18501 (Mar-eco 8445-1), 188.0 mm SL; ZMUB uncat. (Mar-eco 8445-2), 153.5 mm SL.

Leptochilichthys agassizii: BSKU 43180, 298.2 mm SL; ZMUB uncat. (Mar-eco 13309), 133.8 mm SL; ZMUB 18460 (Mar-eco 7325), 259.0 mm SL.

Bathylaco nigricans: ZMUB 18461 (Mar-eco 4401), 254.2 mm SL.

Data availability

The datasets generated and analysed during this study are available from the corresponding author upon request.

Received: 27 April 2018; Accepted: 14 December 2020

Published online: 25 January 2021

References

- Levin, L. A. & Le Bris, N. The deep ocean under climate change. *Science* **350**, 766–768. <https://doi.org/10.1126/science.aad0126> (2015).
- Zarnetske, P. L., Skelly, D. K. & Urban, M. C. Biotic multipliers of climate change. *Science* **336**, 1516–1518. <https://doi.org/10.1126/science.1222732> (2012).
- Tecchio, S. *et al.* Food web structure and vulnerability of a deep-sea ecosystem in the NW Mediterranean Sea. *Deep-Sea Res. Pt. I* (75), 1–15 (2013).
- Clark, A. H. Three interesting additions to the crinoid fauna of Sagami Bay and Suruga Gulf, Japan. *Proc. Biol. Soc. Wash.* **29**, 105–108 (1916).
- Tsujimoto, M. A highly unsaturated hydrocarbon in shark liver oil. *Ind. Eng. Chem.* **8**, 889–896 (1916).
- Shizuoka Prefecture Fisheries Association Management Office. *Shizuoka fisheries report (in Japanese)* (1894).
- Shinohara, G. & Matsuura, K. Annotated checklist of deep-water fishes from Suruga Bay, Japan. *Natl. Sci. Mus. Monogr.* **12**, 269–318 (1997).
- Imajima, M. Polychaetous annelids of Suruga Bay, central Japan. *Natl. Sci. Mus. Monogr.* **12**, 149–228 (1997).
- Takeda, M. Deep-sea decapod crustacean fauna of Suruga Bay, central Japan. *Natl. Sci. Mus. Monogr.* **12**, 229–255 (1997).
- Sazonov, Y. I. A brief review of the genus *Narctes* (Alepocephalidae) with a description of the genus type *N. erimelas*. *J. Ichthyol.* **38**, 491–500 (1998).
- Markle, D. F. *Preliminary studies on the systematics of deep-sea Alepocephaloidea (Pisces: Salmoniformes)* Ph. D. thesis, The College of William and Mary, (1976).
- Nelson, J. S., Grande, T. C. & Wilson, M. V. H. *Fishes of the World* 5th edn. (Wiley, New York, 2016).

13. Froese, R. & Pauly, D. Editors. 2017. FishBase. World Wide Web electronic publication. <http://www.fishbase.org>, version (10/2017).
14. Chakraborty, P., Warren, M., Page, L. M. & Baldwin, C. C. GenSeq: An updated nomenclature and ranking for genetic sequences from type and non-type sources. *Zookeys* **346**, 29–41. <https://doi.org/10.3897/zookeys.346.5753> (2013).
15. Iizuka, K. & Katayama, S. Otolith morphology of teleost fishes of Japan (in Japanese). *Bull. Fish Res. Agen.* **25**, 1–222 (2008).
16. Mindel, B. L., Webb, T. J., Neat, F. C. & Blanchard, J. L. A trait-based metric sheds new light on the nature of the body size–depth relationship in the deep sea. *J. Anim. Ecol.* **85**, 427–436. <https://doi.org/10.1111/1365-2656.12471> (2016).
17. Nielsen, J. M., Popp, B. N. & Winder, M. Meta-analysis of amino acid stable nitrogen isotope ratios for estimating trophic position in marine organisms. *Oecologia* **178**, 631–642. <https://doi.org/10.1007/s00442-015-3305-7> (2015).
18. Heinke, F. Investigations on the plaice. General report 1. The plaice fishery and protective regulations. *Rapp. P.-V. Réun. - Cons. Int. Explor. Mer.* **17**, 1–153 (1913).
19. McClain, C. R. *et al.* Sizing ocean giants: Patterns of intraspecific size variation in marine megafauna. *PeerJ* **3**, e715. <https://doi.org/10.7717/peerj.715> (2015).
20. Timofeev, S. F. Bergmann's principle and deep-water gigantism in marine crustaceans. *Biol. Bull. Russ. Acad. Sci.* **28**, 646–650 (2001).
21. Voorhies, W. A. V. Bergmann size clines: A simple explanation for their occurrence in ectotherms. *Evolution* **50**, 1259–1264 (1996).
22. Collins, M. A., Bailey, D. M., Ruxton, G. D. & Priede, I. G. Trends in body size across an environmental gradient: A differential response in scavenging and non-scavenging demersal deep-sea fish. *Proc. R. Soc. B.* **272**, 2051–2057. <https://doi.org/10.1098/rspb.2005.3189> (2005).
23. Priede, I. G. *Deep-sea Fishes: Biology, Diversity, Ecology and Fisheries* 492 (Cambridge University Press, Cambridge, 2017).
24. Romanuk, T. N., Hayward, A. & Hutchings, J. A. Trophic level scales positively with body size in fishes. *Glob. Ecol. Biogeogr.* **20**, 231–240 (2011).
25. Angulo, A., Baldwin, C. C. & Robertson, D. R. A new species of *Leptoderma* Vaillant, 1886 (Osmeriformes: Alepocephalidae) from the Pacific coast of Central America. *Zootaxa* **4066**, 493–500. <https://doi.org/10.11646/zootaxa.4066.4.10> (2016).
26. Miya, M. & Markle, D. F. *Bajacalifornia aequatoris*, new species of alepocephalid fish (Pisces, Salmoniformes) from the central equatorial Pacific. *Copeia* **1993**, 743–747 (1993).
27. Byrkjedal, I., Poulsen, J. Y. & Galbraith, J. *Leptoderma macrophthalmum* n. sp., a new species of smooth-head (Otocephala: Alepocephalidae) from the Mid Atlantic Ridge. *Zootaxa* **2876**, 49–56 (2011).
28. Carrasson, M. & Cartes, J. E. Trophic relationships in a Mediterranean deep-sea fish community: Partition of food resources, dietary overlap and connections within the benthic boundary layer. *Mar. Ecol. Prog. Ser.* **241**, 41–55 (2002).
29. Mauchline, J. & Gordon, J. D. M. Diets of clupeoid, stomiatoid and salmonoid fish of the Rockall Trough, northeastern Atlantic-Ocean. *Mar. Biol.* **77**, 67–78 (1983).
30. Jones, M. R. L. & Breen, B. B. Food and feeding relationships of three sympatric slickhead species (Pisces: Alepocephalidae) from northeastern Chatham Rise, New Zealand. *Deep-Sea Res. Pt. I* (79), 1–9 (2013).
31. Iken, K., Brey, T., Wand, U., Voigt, J. & Junghans, P. Food web structure of the benthic community at the Porcupine Abyssal Plain (NE Atlantic): A stable isotope analysis. *Prog. Oceanogr.* **50**, 383–405 (2001).
32. Bulman, C. M., He, X. & Koslow, J. A. Trophic ecology of the mid-slope demersal fish community off southern Tasmania, Australia. *Mar. Freshw. Res.* **53**, 59–72. <https://doi.org/10.1071/Mf01057> (2002).
33. Hussey, N. E. *et al.* Expanded trophic complexity among large sharks. *Food Webs* **4**, 1–7. <https://doi.org/10.1016/j.foowe.2015.04.002> (2015).
34. Choy, C. A. *et al.* Global trophic position comparison of two dominant mesopelagic fish families (Myctophidae, Stomiidae) using amino acid nitrogen isotopic analyses. *PLoS ONE* **7**, e50133. <https://doi.org/10.1371/journal.pone.0050133> (2012).
35. Ohkouchi, N. *et al.* A monitoring result of polychlorinated biphenyls (PCBs) in deep-sea organisms and sediments off Tohoku during 2012–2014: Temporal variation and the relationship with the trophic position. *J. Oceanogr.* **72**, 629–639 (2016).
36. Chikaraishi, Y. *et al.* High-resolution food webs based on nitrogen isotopic composition of amino acids. *Ecol. Evol.* **4**, 2423–2449. <https://doi.org/10.1002/ece3.1103> (2014).
37. Barnett, A., Braccini, J. M., Awruch, C. A. & Ebert, D. A. An overview on the role of Hexanchiformes in marine ecosystems: Biology, ecology and conservation status of a primitive order of modern sharks. *J. Fish Biol.* **80**, 966–990. <https://doi.org/10.1111/j.1095-8649.2012.03242.x> (2012).
38. Smale, M. J. Predatory fish and their prey—An overview of trophic interactions in the fish communities of the west and south coasts of South Africa. *S. Afr. J. Mar. Sci.* **12**, 803–821 (1992).
39. Ebert, D. A. Diet of the sixgill shark *Hexanchus griseus* off Southern Africa. *S. Afr. J. Mar. Sci.* **14**, 213–218 (1994).
40. Cortes, E. Standardized diet compositions and trophic levels of sharks. *ICES J. Mar. Sci.* **56**, 707–717 (1999).
41. MacNeill, M. A., Skomal, G. B. & Fisk, A. T. Stable isotopes from multiple tissues reveal diet switching in sharks. *Mar. Ecol. Prog. Ser.* **302**, 199–206. <https://doi.org/10.3354/meps302199> (2005).
42. Chikaraishi, Y. *et al.* Determination of aquatic food-web structure based on compound-specific nitrogen isotopic composition of amino acids. *Limnol. Oceanogr. Methods* **7**, 740–750 (2009).
43. Hannides, C. C. S., Popp, B. N., Landry, M. R. & Graham, B. S. Quantification of zooplankton trophic position in the North Pacific Subtropical Gyre using stable nitrogen isotopes. *Limnol. Oceanogr.* **54**, 50–61. <https://doi.org/10.4319/lo.2009.54.1.0050> (2009).
44. Bowman, R. E. Effect of regurgitation on stomach content data of marine fishes. *Environ. Biol. Fish.* **16**, 171–181 (1986).
45. Reethas, T. *et al.* A new record of Neobythites multistriatus Nielsen & Quéro, 1991 (Ophidiiformes: Ophidiidae) from the Andaman Sea, North Indian Ocean. *Mar. Biodivers.* <https://doi.org/10.1007/s12526-016-0564-4> (2016).
46. Nielsen, J. G., Cohen, D. M., Markle, D. F. & Robins, C. R. *Ophidiiform Fishes of the World (Order: Ophidiiformes)* (FAO, Rome, 1999).
47. Lazzaro, X. A review of planktivorous fishes—Their evolution, feeding behaviors, selectivities, and impacts. *Hydrobiologia* **146**, 97–167. <https://doi.org/10.1007/Bf00008764> (1987).
48. Gerking, S. D. *Feeding Ecology of Fishes* (Academic Press, London, 1994).
49. Janssen, J. Alewives (*Alosa pseudoharengus*) and ciscoes (*Coregonus artedii*) as selective and non-selective planktivores. In *Evolution and Ecology of Zooplankton Communities* (ed. Kerfoot, W. C.) 580–586 (University Press of New England, Lebanon, 1980).
50. Schluter, D. & McPhail, J. D. Ecological character displacement and speciation in sticklebacks. *Am. Nat.* **140**, 85–108. <https://doi.org/10.1086/285404> (1992).
51. Robinson, B. W. & Parsons, K. J. Changing times, spaces, and faces: Tests and implications of adaptive morphological plasticity in the fishes of northern postglacial lakes. *Can. J. Fish. Aquat. Sci.* **59**, 1819–1833. <https://doi.org/10.1139/F02-144> (2002).
52. Kahilainen, K. K. *et al.* The role of gill raker number variability in adaptive radiation of coregonid fish. *Evol. Ecol.* **25**, 573–588. <https://doi.org/10.1007/s10682-010-9411-4> (2011).
53. Shehzad, W. *et al.* Carnivore diet analysis based on next-generation sequencing: Application to the leopard cat (*Prionailurus bengalensis*) in Pakistan. *Mol. Ecol.* **21**, 1951–1965. <https://doi.org/10.1111/j.1365-294X.2011.05424.x> (2012).
54. Sousa, L. L. *et al.* DNA barcoding identifies a cosmopolitan diet in the ocean sunfish. *Sci. Rep.* **6**, 28762. <https://doi.org/10.1038/srep28762> (2016).
55. Dentinger, B. T. M., Didukh, M. Y. & Moncalvo, J. M. Comparing COI and ITS as DNA barcode markers for mushrooms and allies (Agaricomycotina). *PLoS ONE* **6**, e25081. <https://doi.org/10.1371/journal.pone.0025081> (2011).

56. Robideau, G. P. *et al.* DNA barcoding of oomycetes with cytochrome c oxidase subunit I and internal transcribed spacer. *Mol. Ecol. Resour.* **11**, 1002–1011. <https://doi.org/10.1111/j.1755-0998.2011.03041.x> (2011).
57. Sfakiotakis, M., Lane, D. M. & Davies, J. B. C. Review of fish swimming modes for aquatic locomotion. *IEEE J. Oceanic. Eng.* **24**, 237–252. <https://doi.org/10.1109/48.757275> (1999).
58. Webb, P. W. Form and function in fish swimming. *Sci. Am.* **251**, 72–82 (1984).
59. Poulsen, J. Y. *et al.* Preservation obscures pelagic deep-sea fish diversity: Doubling the number of sole-bearing opisthoproctids and resurrection of the genus *Monacoa* (Opisthoproctidae, Argentiniformes). *PLoS ONE* **11**, e0159762. <https://doi.org/10.1371/journal.pone.0159762> (2016).
60. Nagahama, T., Hamamoto, M., Nakase, T., Takaki, Y. & Horikoshi, K. *Cryptococcus surugaensis* sp. nov., a novel yeast species from sediment collected on the deep-sea floor of Suruga Bay. *Int. J. Syst. Evol. Microbiol.* **53**, 2095–2098. <https://doi.org/10.1099/ijs.0.02712-0> (2003).
61. Hasegawa, K. Sunken wood-associated gastropods collected from Suruga Bay, Pacific side of the central Honshu, Japan, with descriptions of 12 new species. *Nat. Sci. Mus. Monogr.* **12**, 59–123 (1997).
62. Saito, H. Deep-sea chiton fauna of Suruga Bay (Mollusca: Polyplacophora) with descriptions of six new species. *Nat. Sci. Mus. Monogr.* **12**, 31–58 (1997).
63. Grekov, A. A. & Pavlenko, A. A. *A Comparison of Longline and Trawl Fishing Practices and Suggestions for Encouraging the Sustainable Management of Fisheries in the Barents Sea* (Index Market Publishing, London, 2011).
64. Estes, J. A. *et al.* Trophic downgrading of planet earth. *Science* **333**, 301–306. <https://doi.org/10.1126/science.1205106> (2011).
65. Baum, J. K. & Worm, B. Cascading top-down effects of changing oceanic predator abundances. *J. Anim. Ecol.* **78**, 699–714 (2009).
66. Wallach, A. D., Ripple, W. J. & Carroll, S. P. Novel trophic cascades: Apex predators enable coexistence. *Trends Ecol. Evol.* **30**, 146–153. <https://doi.org/10.1016/j.tree.2015.01.003> (2015).
67. Sergio, F., Newton, I. & Marchesi, L. Conservation: Top predators and biodiversity. *Nature* **436**, 192. <https://doi.org/10.1038/436192a> (2005).
68. Ripple, W. J. & Beschta, R. L. Trophic cascades in Yellowstone: The first 15 years after wolf reintroduction. *Biol. Conserv.* **145**, 205–213. <https://doi.org/10.1016/j.biocon.2011.11.005> (2012).
69. Myers, R. A., Baum, J. K., Shepherd, T. D., Powers, S. P. & Peterson, C. H. Cascading effects of the loss of apex predatory sharks from a coastal ocean. *Science* **315**, 1846–1850. <https://doi.org/10.1126/science.1138657> (2007).
70. Roff, G. *et al.* The ecological role of sharks on coral reefs. *Trends Ecol. Evol.* **31**, 395–407. <https://doi.org/10.1016/j.tree.2016.02.014> (2016).
71. Pauly, D., Christensen, V. V., Dalsgaard, J., Froese, R. & Torres, F. Jr. Fishing down marine food webs. *Science* **279**, 860–863 (1998).
72. Koslow, J. A. *et al.* Continental slope and deep-sea fisheries: Implications for a fragile ecosystem. *ICES J. Mar. Sci.* **57**, 548–557 (2000).
73. Hartel, K. E. & Orrell, T. M. Alepocephalidae. Slickheads. In *The Living Marine Resources of the Eastern Central Atlantic* Vol. 3 FAO Species Identification Guide for Fishery Purposes (eds K. E. Carpenter & N. De Angelis) 1765–1770 (FAO, Rome, 2016).
74. Sazonov, Y. I. & Markle, D. F. Alepocephalidae. Slickheads. In *The Living Marine Resources of the Western Central Pacific* Vol. 3 FAO Species Identification Guide for Fishery Purposes (eds K. E. Carpenter & V. H. Niem) 1888–1893 (FAO, Rome, 1999).
75. Sazonov, Y. I. On the revision of the genus *Bathytroctes* Günther (Alepocephalidae): A review of the abyssobenthopelagic forms (previously referred to the genus *Nomoctes*) with a description of two new species. *J. Ichthyol.* **39**, 699–712 (1999).
76. Johnson, G. D. & Patterson, C. Relationships of lower euteleostean fishes. In *Interrelationships of Fishes* (eds Stiassny, M. L. J. *et al.*) 251–332 (Academic Press, London, 1996).
77. Markle, D. F. & Merrett, N. R. The abyssal alepocephalid, *Rinoctes nasutus* (Pisces: Salmoniformes), a redescription and an evaluation of its systematic position. *J. Zool.* **190**, 225–239 (1980).
78. Palumbi, S. *et al.* *The Simple Fool's Guide to PCR Version 2.0* (Department of Zoology and Kewalo Marine Laboratory, University of Hawaii, Honolulu, 2002).
79. Folmer, O., Black, M., Hoeh, W., Lutz, R. & Vrijenhoek, R. DNA primers for amplification of mitochondrial cytochrome c oxidase subunit I from diverse metazoan invertebrates. *Mol. Mar. Biol. Biotech.* **3**, 294–299 (1994).
80. Katoh, K. & Standley, D. M. MAFFT multiple sequence alignment software version 7: Improvements in performance and usability. *Mol. Biol. Evol.* **30**, 772–780. <https://doi.org/10.1093/molbev/mst010> (2013).
81. Talavera, G. & Castresana, J. Improvement of phylogenies after removing divergent and ambiguously aligned blocks from protein sequence alignments. *Syst. Biol.* **56**, 564–577 (2007).
82. Castresana, J. Selection of conserved blocks from multiple alignments for their use in phylogenetic analysis. *Mol. Biol. Evol.* **17**, 540–552. <https://doi.org/10.1093/oxfordjournals.molbev.a026334> (2000).
83. Tanabe, A. S. Kakusan4 and Aminosan: Two programs for comparing nonpartitioned, proportional and separate models for combined molecular phylogenetic analyses of multilocus sequence data. *Mol. Ecol. Resour.* **11**, 914–921. <https://doi.org/10.1111/j.1755-0998.2011.03021.x> (2011).
84. Stamatakis, A. RAxML version 8: A tool for phylogenetic analysis and post-analysis of large phylogenies. *Bioinformatics* **30**, 1312–1313 (2014).
85. Leray, M. *et al.* A new versatile primer set targeting a short fragment of the mitochondrial COI region for metabarcoding metazoan diversity: Application for characterizing coral reef fish gut contents. *Front. Zool.* **10**, 34 (2013).
86. Vestheim, H. & Jarman, S. N. Blocking primers to enhance PCR amplification of rare sequences in mixed samples—A case study on prey DNA in Antarctic krill stomachs. *Front. Zool.* **5**, 12. <https://doi.org/10.1186/1742-9994-5-12> (2008).
87. Chikaraishi, Y., Kashiyama, Y., Ogawa, N. O., Kitazato, H. & Ohkouchi, N. Metabolic control of nitrogen isotope composition of amino acids in macroalgae and gastropods: Implications for aquatic food web studies. *Mar. Ecol. Prog. Ser.* **342**, 85–90 (2007).
88. Oguri, K., Yamamoto, M., Toyofuku, T. & Kitazato, H. Developments of deep-sea light and charge pump circuits fixed with an epoxy resin. *JAMSTEC Rep. Res. Dev.* **21**, 7–15. <https://doi.org/10.5918/jamstecr.21.7> (2015).
89. Garman, S. Reports on an exploration off the west coasts of Mexico, Central and South America, and off the Galapagos Islands, in charge of Alexander Agassiz, by the U.S. Fish Commission Steamer Albatross, during 1891, Lieut. Commander Z.L. Tanner, U.S.N., commanding. 26. The fishes. *Memoirs of the Museum of Comparative Zoology at Harvard College, Cambridge, Mass* vol. 24. 1–431 (1899).

Acknowledgements

We thank the captain and crew of the training vessel *Shonan maru* for sampling and baited camera surveys. We also thank Dr. Motoomi Yamaguchi (JAMSTEC) for morphological measurements; Dr. D. Johnson (Smithsonian, U.S.) and Dr. J. Paxton (Australian Museum, Australia) for useful advice; Dr. K-T Shao and Dr. L Y-C Liao (Academia Sinica, Taiwan) and Dr. M. Takami (Tokai University, Japan) for assistance with tissue samples; Ms. Tomomi Nishimura (GE Healthcare Japan) for X-ray tomography scanning observation; Dr. Chong Chen and Dr. Satoshi Okada for producing 3D PDF files and 3D Prints; Dr. Gento Shinohara (National Museum of Nature and Science), Dr. Hiroshi Seno (Kanagawa Prefectural Museum of Natural History), and Drs. Andrew Williston and Meaghan Sorce (Museum of Comparative Zoology) for comparative materials, and Ayaka Takayama,

Yoshimi Umezu, Yasuyuki Matsumoto, and Midori Hagio (JAMSTEC) for research assistance. This work was partly supported by JSPS KAKENHI Grant Number JP16H04611. We would additionally like to thank Editage (<http://www.editage.jp>) for English language editing.

Author contributions

Y.F., M.K., S.T., and S.Ts. collected samples, conducted the baited camera experiment, and conceived the concept of the study. J.Y.P., Y.F., M.K., and H.I. prepared the morphological descriptions. K.O. and S.G. developed the baited camera system. M.K., J.Y.P., M.M., and T.Sa. conducted DNA sequencing. Y.F., M.M., J.Y.P., and G.O. conducted the phylogenetic analyses. M.K. conducted the stomach content analyses. Y.C. and N.O. conducted the nitrogen stable isotope analyses. Y.F., S.Ts., T.T., and K.K. conducted CT analyses. Y.F., M.K., J.Y.P., H.I., and K.K. wrote the manuscript. All the authors reviewed and improved the manuscript.

Competing interests

The authors declare no competing interests.

Additional information

Supplementary Information The online version contains supplementary material available at <https://doi.org/10.1038/s41598-020-80203-6>.

Correspondence and requests for materials should be addressed to Y.F.

Reprints and permissions information is available at www.nature.com/reprints.

Publisher's note Springer Nature remains neutral with regard to jurisdictional claims in published maps and institutional affiliations.



Open Access This article is licensed under a Creative Commons Attribution 4.0 International License, which permits use, sharing, adaptation, distribution and reproduction in any medium or format, as long as you give appropriate credit to the original author(s) and the source, provide a link to the Creative Commons licence, and indicate if changes were made. The images or other third party material in this article are included in the article's Creative Commons licence, unless indicated otherwise in a credit line to the material. If material is not included in the article's Creative Commons licence and your intended use is not permitted by statutory regulation or exceeds the permitted use, you will need to obtain permission directly from the copyright holder. To view a copy of this licence, visit <http://creativecommons.org/licenses/by/4.0/>.

© The Author(s) 2021